TR/08/81 July 1981

Numerical Conformal Mapping of Exterior Domains

N. Papamichael and C.A. Kokkinos*

* On study leave from the National Technical University of Athens,

w926004×

SUMMARY

The work of the present paper is closely related to the two numerical procedures described in [11], for determining approximations to the function which maps conformally a bounded simply-connected domain Ω_1, with boundary $\partial\Omega$, onto the unit disc. Here, we consider the use of these procedures for the solution of the corresponding exterior problem, i.e. the problem of determining approximations to the mapping function which maps conformally the exterior domain $\Omega = \mathrm{compl}(\Omega_1 \cup \partial\Omega)$ onto the unit disc.

1. Introduction

Let Ω_I be a simply-connected domain in the complex z-plane, bounded by a closed Jordan curve $\partial\Omega$, and let ft denote the complement of $\Omega_I \cup \partial\Omega$. This paper is concerned with the problem of determining approximations to the function $w=g(z)$ which maps conformally the exterior domain Ω onto the disc

$$D_R = \{w: |w|<R\} \quad , \tag{1.1}$$

in such a way that $g(\infty)=0$.

We assume, without loss of generality, that the origia 0 is in Ω_I. Then, the inversion

$$\zeta = 1/z \quad , \tag{1.2}$$

transforms $\partial\Omega$ onto a closed Jordan curve $\partial\Omega^*$, and maps conformally the exterior domain Ω onto the interior Ω^* of $\partial\Omega^*$, so that $z=\infty$ corresponds to $\zeta=0$. Let

$$w = f(\zeta) \quad , \tag{1.3}$$

with $f(0)=0$ and $f'(0)=1$, be the conformal transformation of Ω^* onto the disc D_R. Then clearly $w=g(z)$, where

$$g(z) = f(1/z) \quad , \tag{1.4}$$

maps conformally Ω onto the disc D_R so that $g(\infty)=0$. In this way, the problem of determining the exterior mapping function g reduces to that of determining the interior mapping function f for the bounded simply-connected domain Ω^*. We note, in passing, that $w=1/g(z)$ maps conformally Ω onto the exterior of the circle $|w|=1/R$, and that the quantity

$$d = 1/R \quad , \tag{1.5}$$

is the so-called transfinite diameter of $\overline{\Omega}_I = \Omega_I \cup \partial\Omega$ or capacity of the

curve $\partial\Omega$. This quantity plays an important-role in many practical applications ; see e.g. Bergman and Schiffer [2].

In the present paper we determine approximations to f and hence, by means of (1.4), to the exterior mapping function g, by using the two numerical procedures described in [11]. These two procedures involve the numerical implementation of two well-known and closely related methods for conformal mapping. The, two methods are respectively the Ritz method (RM) and the Bergman kernel method (BKM). The RM is a variational method based on the so-called property of minimum area, whilst the BKM is based on the use of the Bergman kernel function of the domain Ω^*. Both methods lead to approximations to $f(\zeta)$, of the form

$$f_n(\xi) = \sum_{j=1}^{n} a_j u_j(\xi) \quad , \tag{1.6}$$

where $\{u_i(\zeta)\}$ is an appropriate set of basis functions.

The theory on which both the RM and the BKM are based is treated extensively in the literature ; see e.g. Bergman [1], Gaier [4] and Nehari [10]. Also, the main theoretical results are summarised in [11]. For this reason, we do not repeat these theoretical details here. Instead, we describe briefly the two methods and indicate the modifications needed for constructing, by means of the procedures of [11], approximations to the exterior mapping function g. In particular, we consider the problem of selecting the set of basis functions $\{u_j(\zeta)$ so that the resulting approximating series (1.6) converges rapidly. For the reasons explained in [9,Sect.2] and [11,Sect.4], the use of such a basis is an essential requirement for the successful application of both the RM and the BKM. In the present paper, as in [11], the basis set is selected by using the process first described, in connection with the BKM, in [9], This process requires knowledge of the dominant singularities

of $f(\zeta)$ in the complement of Ω^*. When this information is available the basis set is constructed by introducing into the monomial set ζ^j ; j=0,1,2,..., functions that reflect the main singular behaviour of $f(\zeta)$.

2. The Numerical Methods

Let $L_2(\Omega^*)$ denote the Hilbert space of all square integrable analytic functions in Ω^*, and let $\{n_j(\zeta)\}$ be a complete set of $L_2(\Omega^*)$. We denote the inner product of $L_2(\Omega^*)$ by $(\ ,\ )$, i.e.

$$(h_1, h_2) = \iint_{\Omega^*} h_1(\xi)\overline{h_2(\xi)}\,ds_\zeta \quad . \tag{2.1}$$

As was previously remarked, the RM is based on the so-called property of minimum area, i.e. the property that the derivative $f'(\zeta)$ of $f(\zeta)$ minimizes uniquely the norm

$$\| u \| = \iint_{\Omega^*} |u(\xi)|^2\, ds_\zeta \quad , \tag{2.2}$$

over all functions $u \in L_2(\Omega^*)$, satisfying $u(0)=1$. More precisely the RM is a variational method for determining approximations to the minimal function $f'(\zeta)$. The details of the method are as follows:

The set $(\eta_j(\zeta))$ is chosen so that

$$\eta_1(0)=1 \quad \text{and} \quad \eta_j(0)=0 \quad ; \quad j=2,3,\ldots, \tag{2.3}$$

and the (n-l)x(n- 1) complex linear system

$$\sum_{j=2}^{n} (n_j, n_i)\, c_j = -(n_j, n_i) \; ; \; i=2,3,\ldots,n \quad , \tag{2.4}$$

is solved for the (n-1) unknowns c_j; $j=2,3,\ldots,n$. Then, the nth RM approximations to the mapping function $f(\zeta)$ and the radius R of the disc D_R are given respectively by

$$f_n(\zeta) = \int_0^{\zeta} \phi_n(t)\, dt \quad , \tag{2.5}$$

and

$$R_n = \| \phi_n \| / \sqrt{\pi} \quad , \tag{2.6}$$

where

$$\phi_n(\zeta) = \eta_1(\zeta) + \sum_{j=2}^{n} c_j \eta_j(\zeta) \quad , \tag{2.7}$$

is the nth RM approximation to $f'(\zeta)$.

Given a complete set $\{\eta_j(\zeta)\}$, the nth BKM approximation to f is obtained by first approximating the Bergman kernel function $K(\zeta;0)$ of Ω^* by a finite Fourier series sum. This kernel function has the reproducing property

$$h(0) = (h,K) \quad , \quad \forall\, h \in L_2(\Omega^*) \quad , \tag{2.8}$$

and is related to the mapping function $f(\zeta)$ by

$$f'(\zeta) = K(\zeta;0)/K(0;0) \quad . \tag{2.9}$$

Also, the radius of the disc D_R is given by

$$R = \{\eta k(0;0)\}^{-\frac{1}{2}} \quad . \tag{2.10}$$

The details of the method are as follows:

The set $\{\eta_j(\zeta)\}^{n}_{j=1}$ is orthonormalized, by means of the Gram-Schmidt process, to give the set of orthonormal functions $\{\eta^*_i(\zeta)\}^{n}_{i=1}$. Then, because of (2.8),

$$K_n(\zeta)0) = \sum_{j=1}^{n} \eta^*_j(0)\, \eta^*_j(\zeta) \quad , \tag{2.11}$$

is the nth partial Fourier sum of the kernel function. Hence, from (2.9) and (2.10), the nth BKM approximations to the mapping function $f(\zeta)$ and the radius R of D_R are given respectively by

$$f_n(\zeta) = \{k_n(0;0)\}^{-1} \int_0^{\zeta} k_n(t;0)\, dt \quad , \tag{2.12}$$

and

$$R = \{\eta k_n(0;0)\}^{-\frac{1}{2}} \quad . \tag{2.13}$$

Let $f_n(\zeta)$ be the nth RM or BKM approximation to $f(\zeta)$. Then, from (1.4), the corresponding nth approximation to the exterior mapping function $g(z)$ is given, quite simply, by

$$g_n(z) = f_n(1/z) \quad , \tag{2.14}$$

The remainder of this section is concerned mainly with the problem of selecting the set of basis functions $\{\eta_j(\zeta)\}$. As was previously remarked this basis set is constructed by introducing into the monomial set

$$\zeta^{j-1}; j = 1, 2, 3, \ldots , \tag{2.15}$$

appropriate functions that reflect the main singular behaviour of $f(\zeta)$ in the complement of Ω^*. The singular functions needed for this purpose are determined, as described in [9,Sect.2] and [1 l,Sect. 4], by considering the poles and branch point singularities of $f(\zeta)$ in compl(Ω^*). However, in our case, the domain $\Omega^*$is obtained from the original unbounded domain Ω by inversion. For this reason, for the problems considered here, it is much more convenient to be able to determine the singularities of $f(\zeta)$ from the geometry of the original boundary $\partial\Omega$.

Let the mapping function $f(\zeta)$ have a simple pole at a point $p^* \in \text{compl}\ (\overline{\Omega^*})$. Then, for the reasons explained in 11 ,Sect.4.1], in order to remove the influence of this pole from the numerical process we augment the set (2.15) by introducing the function

$$\begin{aligned} \eta(\zeta) &= \{\zeta/(\zeta - p^*)\}' + b \\ &= \{-p^*/(\zeta - p^*)^2\} + b \quad , \end{aligned} \tag{2.16}$$

where b=I/p* in the case of the RM, and b=0 in the case of the BKM. Our problem here is to locate the position of the dominant poles of $f(\zeta)$ from the geometry of the original boundary $\partial\Omega$.

As is shown in [9] and [11] the poles of $f(\zeta)$ can always be determined in the case where the boundary $\partial\Omega^*$ of Ω^* consists of straight line segments and circular arcs. If this is so then $f(\zeta)$ has simple poles at the finite inverse (symmetric) points of the origin in the ζ-plane with respect to the straight line segments and to the circular arcs. This can be established, as in [9] and [11] by considering the singularities of the Green's function of Ω^* or, equivalently, by arguments based on the symmetry principle which is discussed, for example, in Henrici [5,p.316]. From the symmetry principle we also know that, under the inversion (1.2), the following two elementary results hold:

(i) A generalized circle Γ in the z—plane is transformed into a generalized circle P* in the ζ-plane. In particular, if Γ is a straight line then Γ^* is a generalized circle passing through the origin of the ζ-plane. (By a generalized circle we mean a curve that is either an ordinary circle or a straight line.)

(ii) Inverse points with respect to the generalized circle Γ in the z-plane are transformed into inverse points with respect to the generalized circle Γ^* in the ζ—plane.

The above observations lead easily to the following results regarding the poles of $f(\zeta)$:

If the original boundary $\partial\Omega$ is a polygon then $f(\zeta)$ has no poles. If $\partial\Omega$ consists of straight line segments and circular arcs then the only poles of $f(\zeta)$ are due to the circular arcs. More precisely, a pole

occurs only if the centre of a circular are is in the interior Ω_I of $\partial\Omega$ and does not coincide with the origin of the z-plane. If $p \in \Omega_I$ is such a centre then $f(\zeta)$ has a simple pole at the point $p^*=1/p \in \text{comp}1\,(\overline{\Omega^*})$.

If the boundary $\partial\Omega$ is more general than a curve consisting of straight line segments and circular arcs then there is no standard technique for determining the poles of $f(\zeta)$. However, as is observed in [9], if a good approximation p^* to the pole at $\zeta=p^*$ can be obtained, by some method, then the introduction of the function

$$\{-\tilde{p}^*/(\zeta-\tilde{p}^*)^2\} + b \quad ,$$

into the set (2,15) is sufficient to remove the influence of the pole from the numerical process.

Branch point singularities are corner singularities. They occur when, due to the presence of a corner at a point $\zeta_0 \in \partial\Omega^*$, the asymptotic expansion of $f(\zeta)$ in the neighbourhood of ζ_0 involves fractional powers of $(\zeta-\zeta_0)$. The question regarding the choice of suitable basis functions for dealing with such singularities can be answered, as in [9] and [11], by using the results of Lehman [8]. This is done quite simply as follows:

Let part of the original boundary $\partial\Omega$ consist of two analytic arcs Γ_1, and Γ_2 which meet at a point z_0 and form there a corner of exterior angle air, where $\alpha=p/q>0$ is a fraction reduced to lowest terms. Then, under the inversion (1.2), Γ_1 and Γ_2 are transformed into two arcs Γ^*_1 and Γ^*_3 which meet at the point $\zeta=1/z_0 \in \partial\Gamma^*$ and form there a corner of interior angle $\alpha\pi$. Because of this, it follows from the results of Lehman [8] that the asymptotic expansion of $f(\zeta)$, in the neighbourhood of ζ_0, involves fractional powers of the form

$$\left.\begin{aligned} &v(\zeta(= (\zeta-\zeta_0)^r - (-\zeta_0)^r \\ \text{where}\quad &r = k + \ell/\alpha \,;\, k = 0, 1, 2, \ldots, \qquad 1 \le \ell \le p \,, \end{aligned}\right\} \tag{2.17}$$

In order to remove the influence of the resulting branch point singularity from the numerical process, we proceed as in [9] and [11] and augment the set (2.15) by introducing the functions

$$\eta(\zeta) - v'(\zeta) - c = r(\zeta - \zeta_0)^{r-1} - c \quad , \tag{2.18}$$

corresponding to the first few singular terms of the sequence (2.17), In (2. 18) $c = r(-\zeta_0)^{r-1}$ in the case of the RM, and $c = 0$ in the case of the BKM.

It should be observed that a branch point singularity might occur at ζ_0 even when $1/\alpha$ is an integer. This happens because the asymptotic expansion of $f(\zeta)$ might involve logarithmic terms of the form

$$(\zeta - \zeta_0)^r \{\log(\zeta - \zeta_0)\}^m \quad , \tag{2.19}$$

where m is a positive integer ; see [8] and [1];Sect,4.2]. However, such logarithmic singularities are never very serious and, for this reason, are not considered further in the present paper.

The evaluation of the coefficients in the linear system (2.4) and the orthonoraalization of the set $\{\eta_j(\zeta)\}$ by means of the Gram-Schmidt process require the evaluation of the inner products

$$(\eta_r, \eta_s = \iint_{\Omega^*} \eta_r(\zeta)\, \overline{\eta_s(\zeta)\, ds_\zeta} \quad ; r, s = 1,2, \ldots, n \quad .$$

Using a Green's formula ([l,p.96],[4,p.118]), the inner products are expressed as

$$(\eta_r, \eta_s = \frac{1}{2i} \int_{\partial\Omega^*} \eta_r(\zeta)\, \overline{\mu_s(\zeta)\, d\zeta} \quad ; \mu_s'(\zeta) = \eta_s(\zeta) \quad ,$$

and hence, by means of (1.2), as

$$(\eta_r, \eta_s = \frac{1}{2i} \int_{\partial\Omega} \frac{1}{z^2}\, \eta_r\left(\frac{1}{z}\right) \overline{\mu_s\left(\frac{1}{z}\right)} dz \quad , \tag{2.20}$$

where the path of integration is in the positive sense with respect to Ω. The contour integrals in (2.20) are then computed by Gaussian quadrature, in exactly the same manner as in [9] and [11]. When performing the quadrature, care must be taken to deal with integrand singularities that occur when, due to the presence of a corner at z_0, the basis set contains singular functions of the form (2.18). If the arms Γ_1 and Γ_2 of the corner are straight line segments then, as explained in [9,Sect.3], such integrand singularities can always be removed by choosing an appropriate parametric representation for $\partial\Omega$.

The computational details concerning the solution of the Hermitian positive definite linear system (2,4) and for performing the orthonormalization of the set $\{\eta_j(0\}$ are exactly as in [11;Sect.5]. That is, the linear system is solved by using the NAG Library routines F01BN and FO4AW, and the orthornormalization is performed by using a procedure based on the standard Gram-Schmidt algorithm.

We end this section by observing that the two methods described above, for computing approximations to the exterior mapping function g(z), admit a more direct interpretation. More precisely, the two methods are equivalent to applying respectively the RM and the BKM, with basis set

$$\theta_j(z) = \{\eta_j(1/z)\}/z^2 \quad ; \; j=1,2,..., \tag{2.21}$$

and inner product

$$\begin{aligned}(\theta_i, \theta_j)_\Omega &= \iint_\Omega \theta_i(z)\,\overline{\theta_j(z)}\,ds_z \\ &= \iint_{\Omega^*} \eta_i(\zeta)\,\overline{\eta_j(\zeta)}\,ds_\zeta = (\eta_i, \eta_j) \quad ,\end{aligned} \tag{2.22}$$

directly to the unbounded domain Ω. This can be deduced easily from the

results of Bergman and Schiffer [2,p.177] and Kantorovich and Krylov [6,p.375]. The reason, for considering the application of the RM and the BKM to the domain Ω^*, rather than to Ω, is that this approach leads easily to the determination of the singular functions needed for constructing the augmented basis.

3. Numerical Examples

In all the examples considered in this section we compute approximations to the mapping function $G(z)$ which maps conformally the exterior domain Ω onto the unit disc

$$D_1 = \{w : |w| < 1\} \quad .$$

These approximations are given by

$$G_n(z) = d_n f_n(1/z) \quad , \tag{3.1}$$

where

$$d_n = 1/R_n \quad , \tag{3.2}$$

is the nth approximation to the transfinite diameter of $\overline{\Omega}_1$. In (3.1) and (3.2), the approximations f_n and R_n are given, in the case of the RM, by (2.5) - (2.7) and, in the case of the BKM, by (2.11) - (2.13).

An estimate of the maximum error in $|G_n(z)|$ is given by the quantity E_n. This is obtained, as in [9] and [11], by computing

$$e_n(z) = 1 - |G_n(z)| \quad , \tag{3.3}$$

at a number of "boundary test points" $z_j \in \partial\Omega$ and then determining

$$E_n = \max_j |e_n(z_j)| \quad , \tag{3.4}$$

In each example, the BKM results presented correspond to the approximation $G_{Nopt}(z)$, where $n = Nopt$ is the "optimum number" of basis functions which gives maximum accuracy in the sense explained in [9] and

[l1] . That is, this number is determined by computing a sequence of approximations $\{G_n(z)\}$, where at each stage the number n of basis functions is increased by one. If at the (n+l) th stage the inequality

$$E_{n+1} < E_n \quad , \tag{3,5}$$

is satisfied then the approximation $G_{n+2}(z)$ is computed When for a certain value of n, due to numerical instability, (3.5) no longer holds then we terminate the process and take n = Nopt. Also, in order to safeguard against slow convergence, after n = 19 we begin to compute the ratios

$$r_M = E_{10+M}/E_M \quad ; M = 10 , 20,..... \quad .$$

If, for some M, $r_M > 0.5$ then we terminate the process at n = 10+M and write $N^*opt = 10+M$.

For the presentation of the results we adopt the format used in [11] . That is, we denote the two methods respectively by RM/MB and BKM/MB or by RM/AB and BKM/AB to indicate whether the "monomial basis" (2.15) or an "augmented basis" is used. For each example we list the singular functions, the boundary test points and the order of the Gaussian quadrature, which are used respectively for augmenting the set (2,15), for determining the error estimate (3.4) and for computing the integrals (2.20). Also, when the accurate computation of the inner products requires the use of a special parametric representation for part of the boundary $\partial\Omega$, we give this representation. In each case the numerical results presented are values of E_{Nopt} , obtained as described above by using (3-4) , and approximations d_{Nopt} to the trasfinite diameter d = 1/ R, computed from (3.2)

In order to simplify the presentation, we use throughout the following notation for representing functions of the form (2.17) - (2.18)

We denote a singular function corresponding to a branch point singularity, due to a fractional power r, at a corner ζ_j of Ω^* by $\eta_{rj}(\zeta)$. That is, $\eta_{rj}(\zeta)$ is defined by

$$\left.\begin{aligned} \eta_{rj}(\zeta) &= v'_{rj}(\zeta) - c_{rj} \quad , \\ v_{rj}(\zeta) &= (\zeta-\zeta_j)^r - (-\zeta_j)^r \quad , \end{aligned}\right\} \tag{3.6}$$

where $c_{rj} = v'_{rj}(0)$ in the case of the RM/AB, and $c_{rj} = 0$ in the case of the BKM/AB.

All computations were carried out on a CDC 7600 computer, using programs written in Fortran with single precision working. Single length working on the CDC 7600 is between 13 and 14 significant figures.

Example 3.1 Exterior of region bounded by the arcs of two intersecting circles ; Figure 3.1.

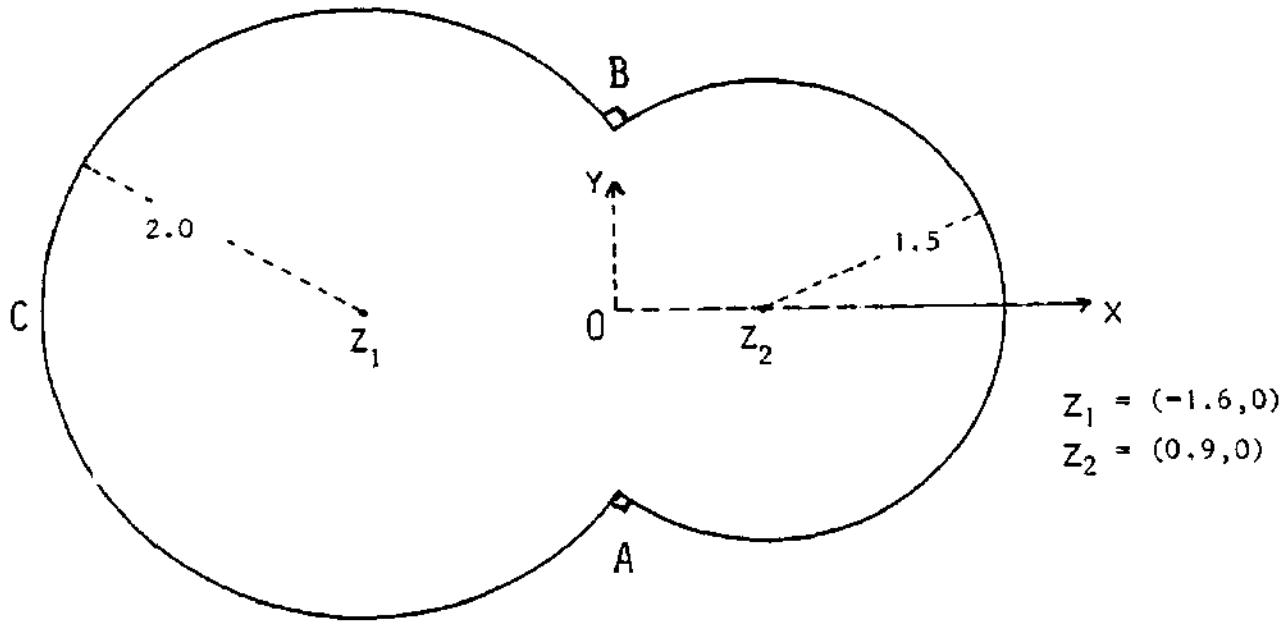

Figure 3.1

Augmented Basis. The following two singular functions, corresponding respectively to the poles of $f(\zeta)$ at the points $\zeta_j = 1/z_j$, $j = 1,2$, are used:

$$\eta_j(\zeta) = v'_{rj}(\zeta) + b_j \quad ; \quad j = 1,2, \tag{3.7}$$

where

$$v_j(\zeta) = \zeta / (\zeta - \zeta_j) \quad ; \quad j = 1, 2, \tag{3-8}$$

$b_j = v'_{rj}(0)$ in the case of the RM/AB, and $b_j = 0$ in the case of the BKM/AB.

Quadrature. Gauss-Legendre formula with 48 points along the arcs AB, BC and CA.

Boundary Test Points, Sixteen points along $\partial\Omega$.

Numerical Results.

BKM/MB : Nopt = 23 , $E_{23} = 1.5\times10^{-4}$, $d_{23} = 2.49999986$.

RM/MB : $E_{23} = 1.3\times10^{-4}$, $d_{23} = 2.49999990$.

BKM/AB : Nopt = 3 = Nmin., $E_3 = 9{,}0\times10^{-14}$, $d_3 = 2{,}5+9.0\times10^{-4}$.

RM/AB : $E_3 = 8.0\times10^{-14}$ $d_3 = 2{,}5+6.0\times10^{-14}$.

In this case the exact mapping function G(z) is

$$G(z) = 2.5z/\{(z-0.9)(z+1.6)\} ;$$

see e.g. Kober [7,p.48]. From this it follows that the exact value of the transfinite diameter is d = 2,5.

The remarkable accuracy achieved by the BKM/AB and RM/AB is due to the fact that

$$G(z) = v_1(1/z) - v_2(1/z) ,$$

where v_j ; $j = 1,2$, are the singular functions (3-8). For this reason the above numerical results are somewhat artificial. They do however illustrate the importance of introducing into the basis set functions that reflect the singular behaviour of $f(\zeta)$.

Example 3.2. Exterior of rectangle ; Figure 3.2.

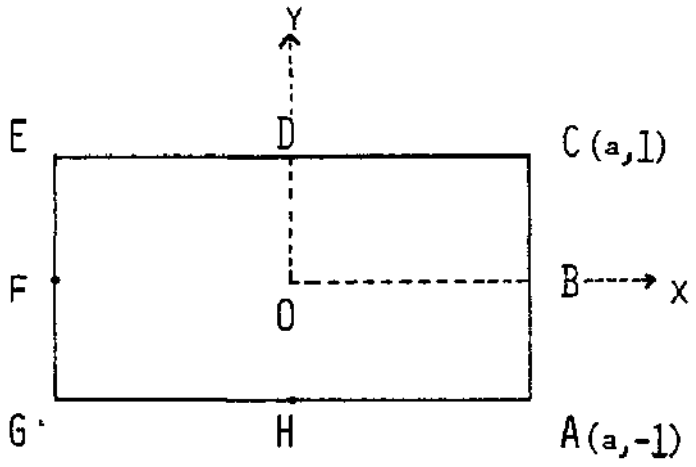

Figure 3.2

Augmented Basis. When a = 1 the domain has eightfold symmetry about the origin and, because of this, the monomial basis set used for the approximation of $f'(\zeta)$ and $K(\zeta;0)$ is taken to be

$$\zeta^{4(j-1)} \; ; \; j = 1,2,3,\ldots \quad . \tag{3.9}$$

Similarly, when $a \neq 1$ the domain has fourfold symmetry and the monomial set is taken to be

$$\zeta^{2(j-1)} \; ; \; j = 1,2,3,\ldots \quad . \tag{3.10}$$

Let z_j ; j = 1,2,3,4 be respectively the corners A, C, E and G of the rectangle. Then, the singular functions corresponding to the branch point singularities at the corners $\zeta_j = 1/z_j$; j = 1,2,3,4 of Ω^* are respectively the functions $\eta_{rj}(\zeta)$; j = 1,2,3,4, given by (3.6) with

$$r = k + 2\ell/3 \; ; \; k = 0,1,2,\ldots \; , \; 1 \leq \ell \leq 3,$$

When a = 1 the symmetry of the domain implies that, for each value of r, the four functions $\eta_{rj}(\zeta)$ can be combined into the single function

$$\left.\begin{aligned} H_r(\zeta) &= v_r'(\zeta) - c_r \quad , \\ v_r(\zeta) &= v_{rl}(\zeta) + \sum_{j=2}^{4} e^{i\theta j} v_{rj}(\zeta) \quad , \end{aligned}\right\} \tag{3.11}$$

where the arguments θ_j ; j = 2,3,4, are chosen so that

$$V_r(e^{i\pi/2}\zeta) = e^{i\pi/2}\, v_r(\zeta)\,. \tag{3.12}$$

Similarly, if $a \neq 1$ then for each value of r the four functions $\eta_{rj}(\zeta)$ can be combined into the two functions

$$\left.\begin{aligned} H_{rj}(\zeta) &= v_r'(\zeta) - c_{rj} \quad , \\ v_{rj}(\zeta) &= v_{rj}(\zeta) + e^{i\phi j} v_{r,j+2}(\zeta) \;;\; j = 1,2 \,, \end{aligned}\right\} \tag{3.13}$$

where, in this case, the arguments ϕ_j ; j = 1,2, are chosen so that

$$V_{rj}(e^{i\pi}\zeta) = e^{i\pi} V_{rj}(\zeta). \tag{3.14}$$

The constants C_r and C_{rj} in (3.11) and (3.13) are respectively $C_r = V'_r(0)$ and $C_{rj} = v'_{rj}(0)$ in the case of the RM/AB, and $C_r - C_{rj} = 0$ in the case of the BKM/AB.

It is important to observe that the constants θ_j and ϕ_j in (3.11) and (3.13), depend on the branches used for defining the functions $v_{rj}(\zeta)$. For this reason, great care must be taken when constructing symmetric singular functions of the form (3.11) or (3.13).

In this example we form the augmented basis, for the cases a = 1 and $a \neq 1$, by introducing respectively into the monomial sets (3.9) and (3.10) the functions (3.11) corresponding to the three values r = 2/3, 4/3, 5/3, and the functions (3,13) corresponding to the four values r = 2/3, 4/3, 5/3, 7/3.

Quadrature. Gauss-Legendre formula with 48 points along AB, BC, ...,HA.

In order to perform the integration, accurately we choose the parametric representations of BC,CD,...,AB to be

$$z = \begin{cases} (z_B - z_C)\,(1-\tau)^3 + z_C\,, & 0 \le \tau \le 1 \;\text{; for BC,} \\ (z_D - z_C)\,(\tau-1)^3 + z_C\,, & 1 \le \tau \le 2 \;\text{; for CD,} \\ (z_D - z_E)\,(3-\tau)^3 + z_E\,, & 2 \le \tau \le 3 \;\text{; for DE,} \\ \cdots\cdots\cdots\cdots\cdots\cdots \\ \cdots\cdots\cdots\cdots\cdots\cdots \\ z_B - z_A)\,(\tau-7)^3 + z_A\,, & 7 \le \tau \le 8 \;\text{; for AB,} \end{cases}$$

Boundary Test Points. Because of the symmetry, we only consider points on AC and CE. The points are distributed in steps of 0,2 and a/5 along AC and CE respectively, starting from A,

Numerical Results.

(i) a = 1

BKM/MB : N_0^*pt = 20, $E_{20} = 8.0 \times 10^{-2}$, $d_{20} = 1.1731$

BKM/AB : Nopt = 21, $E_{21} = 1.2 \times 10^{-6}$, $d_{21} = 1.18034059900.$

RM/AB : $E_{21} = 3.3 \times 10^{-6}$, $d_{21} = 1.18034059934.$

Exact value of d = 1.18034059902.

(ii) a = 2

BKM/MB : N_0^*pt = 20, $E_{20} = 1.4 \times 10^{-1}$, $d_{20} = 1.7163\ldots\ldots..$

BKM/AB : Nopt = 17, $E_{17} = 8.6 \times 10^{-6}$, $d_{17} = 1.7495345562.$

RM/AB : $E_{17} = 1.1 \times 10^{-5}$, $d_{17} = 1.7495145557.$

Exact value of d = 1,7495145563.

(iii) a = 6

BKM/MB : N_0^*pt = 20, $E_{20} = 5.6\ 10^{-1}$, $d_{20} = 2.528\ldots\ldots\ldots$

BKM/AB : Nopt = 15, $E_{15} = 3.8\ 10^{-4}$, $d_{15} = 3.8831423.$

RM/AB : $E_{15} = 3.8\ 10^{-4}$, $d_{15} = 3,8831423.$

Exact value of d = 3.8831450.

The exact values of the transfinite diameter d, listed above, were

computed by using the exact formula of Bickley [3 ,p.86].

Example 3.3. Exterior of equilateral triangle ; Figure 3.3.

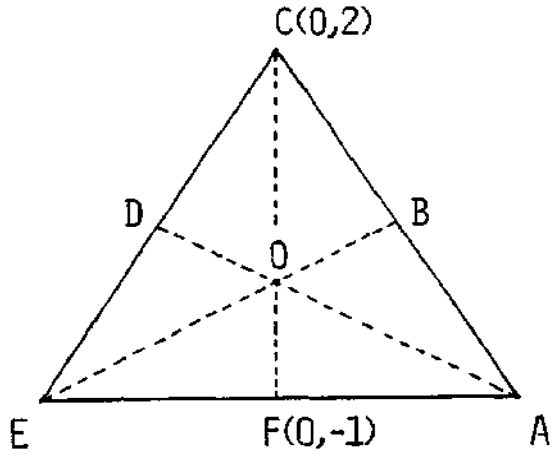

Figure 3.3

Augmented Basis, Because the domain has sixfold symmetry about the origin, the monomial basis used for the approximations of f'(ζ) and K(ζ ;0) is taken to be

$$\zeta^{3(j-1)} ; j = 1,2,3,\ldots \quad . \tag{3.15}$$

Let z_j ; j = 1,2,3, be respectively the corners A,C and E of the triangle. Then, the singular functions corresponding to the branch point singularities at the corners $\zeta_{.j} = 1/z_j$; j = 1,2,3 of Ω* are respectively the functions $\eta_{rj}(\zeta)$; j = 1,2,3, given by (3.6) with

$$r = k + 3/5 \quad ; \quad k = 0, 1, \ldots , 1 < \ell < 5.$$

Because of the symmetry, for each value of r, the three functions $\eta_{rj}.(\zeta)$ can be combined into the single function

$$\left.\begin{aligned} H_r(\zeta) &= v_r'(\zeta) - c_r \quad , \\ v_r(\zeta) &= v_{rl}(\zeta) + \sum_{j=2}^{3} e^{i\theta j} v_{rj}(\zeta) \quad , \end{aligned}\right\} \tag{3.16}$$

where the arguments 9. are chosen so that

$$V_r(e^{2\pi i/3}\zeta) = e^{2\pi i/3} V_r(\zeta) \quad .$$

The augmented basis is formed by introducing into the set (3.15) the four singular functions (3. 16) corresponding to the values r = 3/5, 6/5, 8/5, 9/5.

Quadrature. Gauss-Legendre formula with 48 points along AB,BC,.....,FA.

In order to perform the integration accurately we choose the parametric representations of $BC, CD, \ldots, AB$ to be

$$z = \begin{cases} (z_B - z_C)\,(1-\tau)^5 + z_C\,, & 0 \le \tau \le 1 \ ; \text{ for BC,} \\ (z_D - z_C)\,(\tau-1)^5 + z_C\,, & 1 \le \tau \le 2 \ ; \text{ for CD,} \\ (z_D - z_E)\,(3-\tau)^5 + z_E\,, & 2 \le \tau \le 3 \ ; \text{ for DE,} \\ \cdots\cdots\cdots & \\ z_B - z_A)\,(\tau-7)^3 + z_A\,, & 7 \le \tau \le 6 \ ; \text{ for AB,} \end{cases} \qquad (3.17)$$

Boundary Test Points. Because of the symmetry we only consider nine points on BCD. The distribution of these points is defined by (3.17) with $\tau = 0\ (0.5)2$.

Numerical Results.

BKM/MB : N_0^* opt = 20, $E_{20} = 2.7X10^{-1}$, $d_{20} = 1.399.....$

BKM/AB : Nopt = 13, $E_{13} = 3.2x10^{-5}$, $d_{13} = 1,46099857.$

RM/AB : $E_{13} = 3,3x10^{-5}$, $d_{13} = 1,46099855,$

Exact value of d = 1,46099849,

The exact value of d, listed above, was computed by using the exact formula of Pólya and Szegö [12 p.256].

Example 3.4. Exterior of L-shaped region ; Figure 3.4.

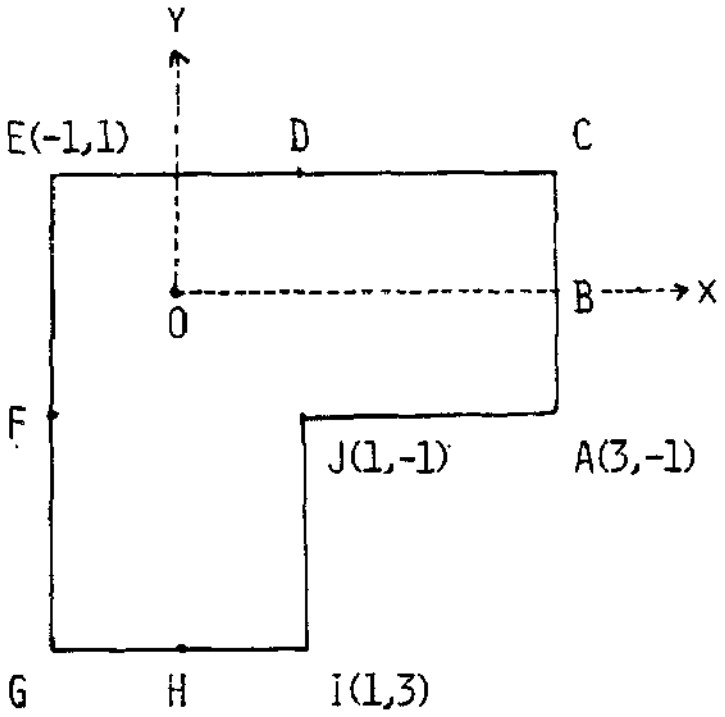

Figure 3.4

Augmented Basis. Let z_j ; $j = 1,2,3,4,5$, be respectively the corners A, C, E, G and I, Then the singular functions corresponding to the branch point singularities at the corners $\zeta_j = 1/z_j$; $j = 1,2,3,4,5$ of Ω^* .are respectively the functions $\eta_{rj}(\zeta)$; $j = 1,2,3,4,5$, given by (3.6) with

$$r = k + 2\ell/3 \quad ; \; k = 0,1,2, \ldots, \quad 1 \leq \ell \leq 3.$$

The augmented basis is formed by introducing into the set (2.15) the twenty singular functions corresponding to the values r = 2/3, 4/3, 5/3, 7/3,

Quadrature. Gauss-Legendre formula with 48 points along AB,BC,..,JA.

In order to perform the integration accurately we choose the

parametric representations of $BC, CD, \ldots, AB$ to be

$$z = \begin{cases} (z_B - z_C)^3\ (1-\tau)^3 + z_C\ , & 0 \le \tau \le 1\ ;\ \text{for BC}, \\ (z_D - z_C)\ (1-\tau)^3 + z_C\ , & 1 \le \tau \le 2\ ;\ \text{for CD}, \\ \cdot \quad \cdot \quad \cdot \quad \cdot \quad \cdot \quad \cdot & \\ \cdot \quad \cdot \quad \cdot \quad \cdot \quad \cdot \quad \cdot & \\ z_B - z_A)\ (\tau - 9) + z_A\ , & 9 \le \tau \le 10\ ;\ \text{for AB}, \end{cases} \tag{3.18}$$

Boundary Test Points. The distribution of the points is defined by (3.18) with $\tau = 0(0.25)\ 10$,

Numerical Results,

BKM/MB : $N_0^* pt = 20$, $E_{20} = 2.7 \times 10^{-1}$, $d_{20} = 2.0493$

BKM/AB : Nopt = 29, $E_{29} = 4.3 \times 10^{-5}$, $d_{29} = 2.1697807486$,

RM/AB : $E_{29} = 4.4 \times 10^{-5}$, $d_{29} = 2.1697807485$,

Example 3.5. Exterior of cross shaped region ; Figure 3.5.

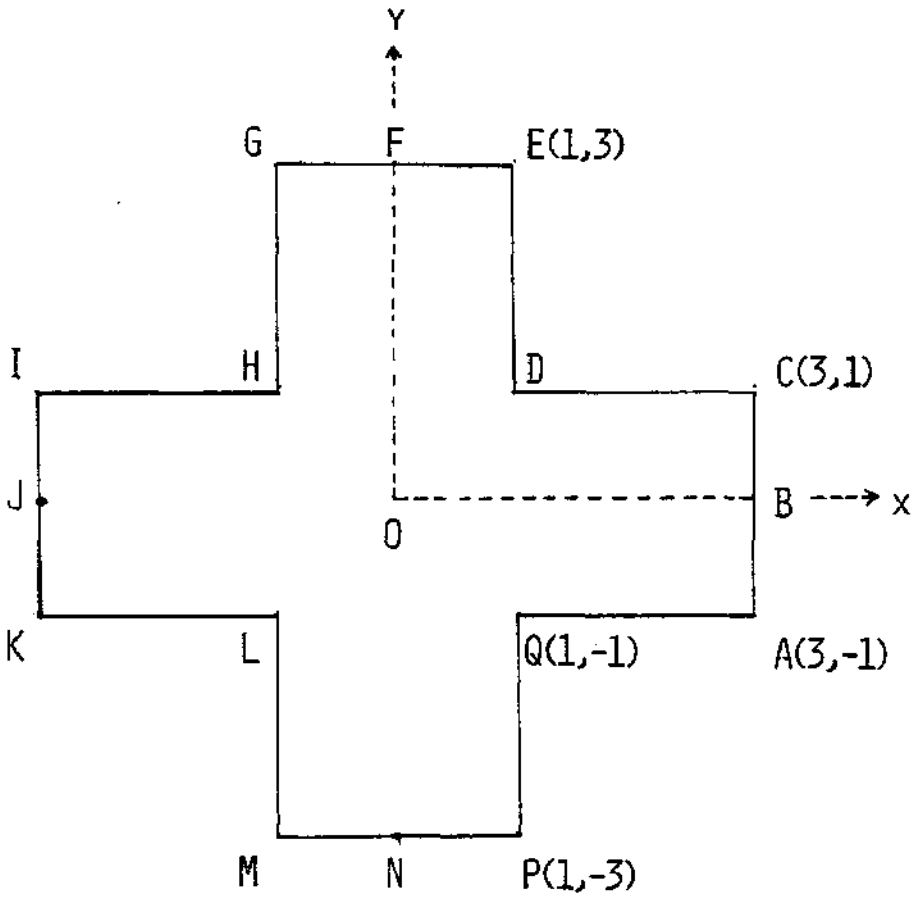

Figure 3,5

Augmented Basis. Because the domain has eightfold symmetry about the origin, the monomial set is taken to be the set (3.9).

Let z_j ; j = 1,2,...,8 be respectively the corners A, C, E, G, I, K, M and P, Then, the singular functions corresponding to the branch point singularities $\zeta_j = 1/z_j$; j = 1, 2,....,8 of Ω^* are respectively the functions $\eta_{rj}(\zeta)$; j = 1,2,...,8, given by (3.6) with

$$r = k + 2\ell/3 \quad ; k = 0,1,2,\ldots, 1 \le \ell \le 3,$$

Because of the symmetry, for each value of r, the eight singular functions can be combined into the two functions

$$\left.\begin{aligned} H_{rj}(\zeta) &= v_r'(\zeta) - c_{rj} \quad , \\ v_{rj}(\zeta) &= v_{rj}(\zeta) + \sum_{j=1}^{3} e^{i\theta 2m+j} v_{r,2m+j}(\zeta) \; ; \; j = 1,2, \end{aligned}\right\} \tag{3.19}$$

where, as in (3.11), the arguments θ_{2m+j} are chosen so that

$$V_{rj}(e^{i\pi/2}\zeta) = e^{i\pi/2} v_{rj}(\zeta) \; .$$

The augmented basis is constructed by introducing into the set (3,8) the six singular functions of the form (3,17), corresponding to the values r - 2/3, 4/3, 5/3.

Quadrature. Gauss-Legendre formula with 48 points along AB,BC,....,QA.

In order to perform the integration accurately we choose the parametric representations of BC,CD,....,AB, to be

$$z = \begin{cases} (z_B - z_C)(1-\tau)^3 + z_C \; , \; 0 \le \tau \le 1 \; ; \text{ for BC}, \\ (z_D - z_C)(\tau - 1)^3 + z_C \; , \; 1 \le \tau \le 2 \; ; \text{ for CD}, \\ \cdot \quad \cdot \quad \cdot \quad \cdot \quad \cdot \quad \cdot \\ \cdot \quad \cdot \quad \cdot \quad \cdot \quad \cdot \quad \cdot \\ z_B - z_A)(\tau - 15)^3 + z_A \; , \; 15 \le \tau \le 16 \; ; \text{ for AB}, \end{cases} \tag{3.20}$$

Boundary Test Points, Because of the symmetry we only consider seventeen points on BCDEF. The distribution of these points is defined by (3,19) with $\tau = 0(0.25)4$.

Numerical Results.

BKM/MB : N_0^*pt = 20 , $E_{20} = 1.2\times10^{-1}$, $d_{20} = 2.7813$

BKM/AB : Nopt = 12 , $E_{12} = 3.5\times10^{-5}$, $d_{12} = 2.85137\ 11607.$

RM/AB : $E_{12} = 3.5\times10^{-5}$, $d_{12} = 2,8513711605.$

4. Conclusions

The results given in Section 3 indicate clearly that both the RM and the BKM are capable of producing approximations of high accuracy for the mapping of "difficult" exterior domains. As in the case of the interior mapping problem, the essential requirement for this is that the basis set contains appropriate singular functions.

Regarding computational efficiency, our experiments here confirm the conclusions reached in [11], for the interior problem. That is, the two methods require the same computational effort for producing approximations of comparable accuracy.

We are grateful to Dr. D. Levin for many valuable discussions during the work described above. We are also grateful to Professor D. Gaier whose detailed comments on the original draft of the manuscript improved the presentation of the paper.

REFERENCES

[1] S. Bergman, The kernel function and conformal mapping, Math. Surveys, No 5, 2nd edition, (Amer. Math. Soc, Providence, R.I., 1970).

[2] S. Bergman and M. Schiffer, Kernel functions and elliptic differential equations in mathematical physics. (Academic Press, New York 1953).

[3] W.G. Bickley, Two—dimensional potential problems for the space outside a rectangle, Proc. Lond. Math. Soc., Ser. 2, 37 (1932) 82 - 105.

[4] D. Gaier, Konstruktive Methoden der konformen Abbildung (Springer-Verlag, Berlin 1964).

[5] P. Henrici, Applied and computational complex analysis, Vol. 1. (Wiley, New York 1974).

[6] L. V. Kantorovich and V.I. Krylov, Approximate methods of higher analysis (Interscience. New York 1964).

[7] H. Kober, Dictionary of conformal representations, (Dover, New York 1957).

[8] R. S. Lehman, Development of the mapping function at an analytic corner, Pacific J. Math. 7 (1957) 1437 - 1449.

[9] D. Levin, N. Papamichael and A. Sideridis, The Bergman kernel method for the numerical conformal mapping of simply-connected domains, J. Inst. Maths Applies, 22 (1978) 171 - 187.

[10] Z. Nehari, Conformal mapping (McGraw-Hill,New York 1952).

[11] N. Papamichael and C.A . Kokkinos, Two numerical methods for the conformal mapping of simply-connected domains. To appear in: Comput, Me ths App1. Mech. Engrg.

[12] G. Polya and G. Szego, Isoperimetric inequalities in mathematical physics. (Princeton University, 195 1).